

Comparative Study on Tool Fault Diagnosis Methods Using Vibration Signals and Cutting Force Signals by Machine Learning Technique

Suhas S. Aralikatti¹, K. N. Ravikumar¹, Hemantha Kumar^{1,*}, H. Shivananda Nayaka¹ and V. Sugumaran²

¹National Institute of Technology Karnataka, Mangaluru, 575 025, India

²Vellore Institute of Technology University, Chennai, 600 127, India

*Corresponding Author: Hemantha Kumar. Email: hemanta76@gmail.com

Received: 10 June 2019; Accepted: 15 July 2019

Abstract: The state of cutting tool determines the quality of surface produced on the machined parts. A faulty tool produces poor surface, inaccurate geometry and non-economic production. Thus, it is necessary to monitor tool condition for a machining process to have superior quality and economic production. In the present study, fault classification of single point cutting tool for hard turning has been carried out by employing machine learning technique. Cutting force and vibration signals were acquired to monitor tool condition during machining. A set of four tooling conditions namely healthy, worn flank, broken insert and extended tool overhang have been considered for the study. The machine learning technique was applied to both vibration and cutting force signals. Discrete wavelet features of the signals have been extracted using discrete wavelet transformation (DWT). This transformation represents a large dataset into approximation coefficients which contain the most useful information of the dataset. Significant features, among features extracted, were selected using J48 decision tree technique. Classification of tool conditions was carried out using Naïve Bayes algorithm. A 10 fold cross validation was incorporated to test the validity of classifier. A comparison of performance of classifier was made between cutting force and vibration signal to choose the best signal acquisition method in classifying tool fault conditions using machine learning technique.

Keywords: Fault diagnosis of cutting tool; Naïve Bayes classifier; decision tree technique

1 Introduction

Condition monitoring of cutting tool is necessary to ensure efficient machining operation with minimal tooling costs and minimal down time. Tool condition monitoring (TCM) in machining is essential to predict tool wear and kind of surface finish produced on workpiece. Tool fault diagnosis is one method of TCM. Tool wear estimation by conventional Taylor's tool life equation is prone to either underestimation or overestimation [1]. Excessive replacement of tool leads to huge tooling cost. Consequently, valuable resource and precious time are at stake [2]. Most down time in machining is caused due to tool breakage



This work is licensed under a Creative Commons Attribution 4.0 International License, which permits unrestricted use, distribution, and reproduction in any medium, provided the original work is properly cited.

and tool handling. The only technique that is viable in reducing the down time during machining is Tool Condition Monitoring (TCM). TCM involves monitoring tool health status by acquiring real time tool condition information using sensors and transducers such as accelerometer [3–5], dynamometer [6], acoustic emission (AE) sensor [7], current sensor [8], surface profiler [9], pyrometer [10] and charge coupled device (CCD) camera [11]. The sensor data will be in raw form or in time-domain, which is not in information revealing form. These sensor data have to be processed to improve subjective quality and to detect components of interest in a measured signal [12]. Various signal processing techniques used by researchers include; Fourier transform, short time Fourier transform, wavelet transform, etc., However, to make the condition monitoring automatic, precise and accurate the monitoring has to happen online. The condition of fault would be many in numbers. In such cases the monitoring system has to learn from the previous experience and be able to recognize the fault in the system as and when they occur. This pre recorded (by previous experience) faulty conditions serve as signature signals which act as reference for fault identification during actual running condition.

Tool condition monitoring can be carried out either by direct measurement or by indirect measurement. Non-contact, direct measurement of cutting tool edges with sophisticated systems give accurate information about tool wear. Jurkovic et al. [13] used CCD camera to create 3D image of relief surface to measure tool wear of carbide inserts. The technique had the characteristic of measuring the profile depth with the help of projected lased light using a diode and linear projector. Uehara et al. [14] used laser sensor which reconstructs 3D image of milling tool profile with laser displacement and intensity technique to evaluate geometric failures of tool. The technique was able to detect the location of tool chipping and length of flank wear at an accuracy of 40 micron. Schmitt et al. [15] employed machine vision system to measure tool wear and classify them by neural network based on active contour algorithm. Tools were held in special fixture for image acquisition of tool wear. Image processing chain comprised feature extraction, classification and tool wear measurement. Ramirez-Nunez et al. [16] used infrared thermography to monitor tool breakage during milling process under dry condition and wet conditions. Healthy state or broken state of a tool is determined by analysing temperature gradients in the cutting zone. Direct measurement yields accurate readings only in limited condition. However, cutting fluid, surrounding the tool, forms the barrier for direct measurement. Nowadays, indirect method of tool wear monitoring is found to be more effective for online monitoring of machining operation with advancement of signal processing, image processing and artificial intelligence.

Indirect measurement method uses sensors and transducer signals such as force signal, vibration signals, Acoustic Emission (AE) signals, current signatures and temperature readings. Acquired signals are raw in nature, which need to be processed to understand the hidden information about the ailment in the system. Dimla [17] followed experimental and analytical methods to correlate tool wear with measured vibration signal and cutting force signal independently for turning operation. It was found that z-direction of cutting force and vibration signal were sensitive to the tool wear. Hesser et al. [18] retrofitted an old CNC milling machine to monitor tool wear by embedding programmable sensor (Bosch XRD sensor platform) which sends vibration information of machining process through wireless communication mode. Two tool condition healthy and worn tool were considered for the study. Tool state classification was carried out using machine learning approach. Various machine learning techniques were used to classify tool state. Score, recall and precision evaluated performance of these models. Liu et al. [19] applied signal-processing techniques such as time domain analysis, Fast Fourier Transform (FFT) analysis and wavelet decomposition method for both vibration signal and cutting force signal corresponding to milling of thin wall feature to recognise the complex machining condition. Bhuiyan et al. [20] carried out experimental investigation to monitor tool abrasion, surface finish and chip formation using accelerometer and acoustic emission sensors in turning operation. Plaza et al. [21] monitored on-line surface roughness of finish turning operation on CNC lathe by applying singular spectrum analysis to vibration signal acquired during machining operation.

Various machine learning techniques followed in literature to monitor various systems include neural networks, fuzzy logic and artificial intelligence. Understanding deep hidden information in a signal is achieved by extracting remarkable features such as Discrete Wavelet Transform (DWT) features, statistical features, histogram features, etc. Further, significant features among extracted features are selected and fault conditions are classified. Salgado et al. [22] estimated surface roughness for turning operation using support-vector machine. Kannatey et al. [23] adopted classifier fusion technique to improve tool wear monitoring for coroning process (a finishing operation). Cuka et al. [24] performed embedded tool condition monitoring of end milling tool with the signals acquired from dynamometer, microphone, accelerometer and current sensor using machine learning technique. Sugumaran et al. [25] used decision tree to monitor health condition of roller bearing using vibration signal. Features of vibration signal were deduced using statistical analysis. Elangovan et al. [26] compared fault classification based on feature selection using J48 algorithm and principal component analysis to monitor turning tool using vibration information.

Force and vibration signals are used for tool fault detection, tool chatter detection, due to the complex relationship that exists between vibrations, cutting force and process dynamics. Several researchers presented machine learning techniques on various machining processes and found it effective in diagnosing the machining faults. However, none have reported use of cutting force for turning operation with machine learning technique despite its advantages. Hence, there is a need to study the tool condition monitoring using cutting force signal in conjunction with machine learning technique for tool fault diagnosis. Cutting force provide thorough insight into tool fault diagnosis. In this article, we attempt to compare the performance on classification of tool faults carried out using both vibration and cutting force signal with machine learning technique applied. Healthy and three faulty condition of tool were considered for the current study. The classifier was verified using 10 fold cross validation with 66% of total data as training data set and remaining as test data.

2 Methodology

Sequential steps followed for fault diagnosis of single point cutting tool during hard turning is shown in Fig. 1. Both healthy and simulated faulty tools were used for machining oil hardened nickel steel workpiece. Cutting force signals and vibration signals were acquired using cutting tool dynamometer and accelerometer. Pre-processing of signal was carried out independently for each signal type in order to feed to the transformation tool. Discrete wavelet features were extracted from the signals through discrete wavelet transform (DWT) which was a MATLAB code. DWT yields 8 wavelet coefficients (features) for each single second data. Significant features are selected from the coefficients yielded by DWT. This selection of significant features was made by J48 decision tree algorithm. The tree represents the significant features for classification in pictorial form with logic of classification visible explicitly. Decision tree can be used as feature selector as well as classifier if, it provides good classification accuracy else, different other classifiers tested to classify the tool conditions. In this paper, Naïve Bayes algorithm was used to classify the tool faults. Since two signal types are used, the classification accuracy obtained with vibration and cutting force signal were compared to see which sensor signal is more suitable for tool fault classification.

3 Machine Learning Applied to Machining Process

Machine learning aims at development of computer programs in the form of models. These models can get access to data and find patterns in them to learn automatically. Learning starts with examinations of given data. The objective of examining the data is to watch for trends in data and make suitable decisions for the new data based on the trained examples. The prime intention to do so is to allow the computers, learn for themselves and adjust parameters of model accordingly [27].

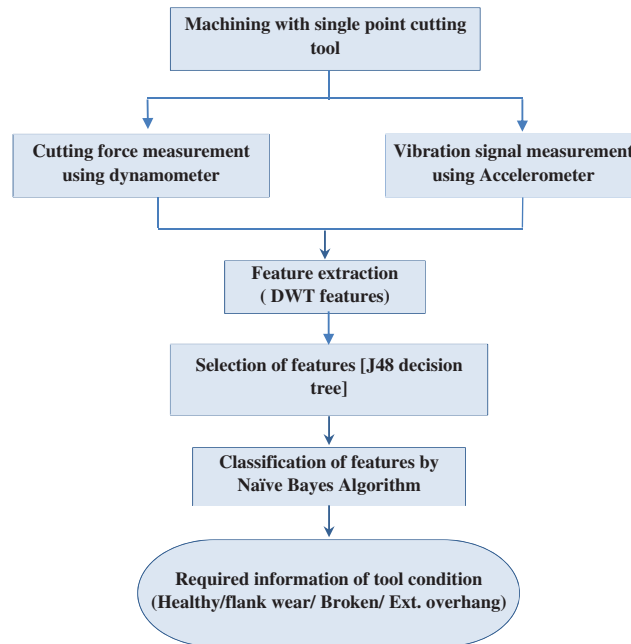


Figure 1: Methodology followed to classify tool faults using machine learning technique

3.1 Wavelet Transform Analysis

Wavelet as a mathematical tool used to divide a continuous-time signal into different scale components. The wavelets are scaled and translated over a finite-length waveform. This finite length waveform is known as mother wavelet and scalable and translatable wavelets are called daughter wavelets. Wavelet transforms can represent functions that have discontinuities and sharp peaks. Wavelet transformation deconstructs and reconstructs non-stationary signals accurately, where traditional Fourier transform fails to do so [28–29].

Wavelet transforms is used to transform data, then encode the transformed data. Wavelet transforms can be of two types. First, discrete wavelet transforms (DWTs); second, continuous wavelet transforms (CWTs). DWTs use a specific subset of scale and translation values. CWTs operate over every possible scale and translation and CWT are generally used for signal analysis [30–31].

3.1.1 Feature Extraction Using Discrete Wavelet Transform

The effective way of representing large data (signal) is achieved by correlating with approximation coefficients. These coefficients contain most useful information of dataset [32]. Decomposed signal has detail coefficients and approximation coefficients. Detailed coefficients describe high-frequency coefficients while approximation coefficients describe low-frequency coefficients [33]. Approximation coefficients will be considered in each feature vector for the formation of the vector which is shown in pictorial form in Fig. 2. Feature V1 is level one decomposition. V2 is level two decomposition and so on.

Wavelet considered for present study is Haar wavelet. Haar low pass filter computes simple average while Haar high pass filter computes simple difference. The basis function for the DWT are the filter coefficients.

The DWT feature vector is given by,

$$v^{dwt} = \{v_1^{dwt}, v_2^{dwt}, \dots, v_n^{dwt}\}^T \quad (1)$$

v_i^{dwt} is the element associated to the different resolutions and can be calculated as follows,

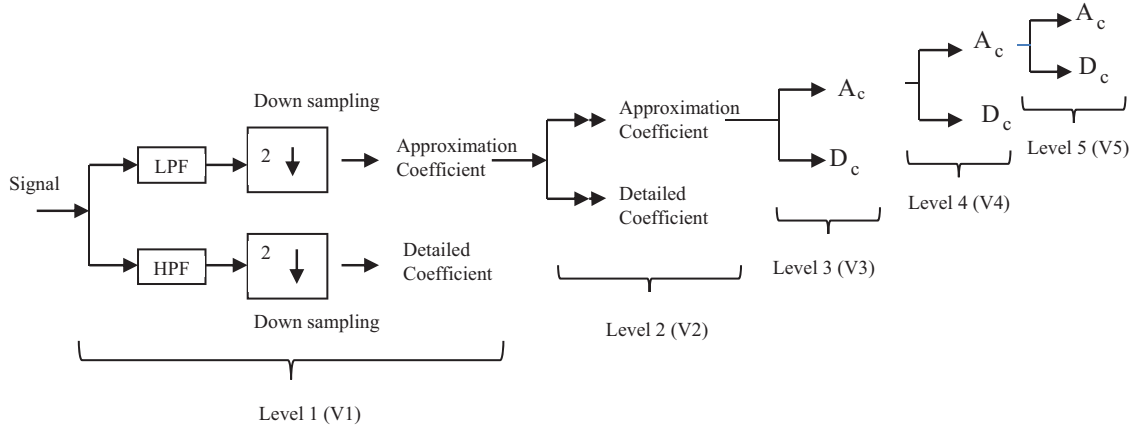


Figure 2: Signal decomposition to obtain approximation coefficient and detailed coefficient

$$v_i^{dwt} = \frac{1}{n_i} \sum_{j=1}^{n_i} W_{ij}^2; i = 1, 2, \dots, 8 \quad (2)$$

$$n_1 = 2^8, n_2 = 2^7, \dots, n_8 = 2^0 \quad (3)$$

v_i^{dwt} is i^{th} feature vector element in DWT vector,

n_i is the number of samples in the sub band,

w_{ij}^2 is the sub band for the j^{th} detailed coefficient.

DWT has different wavelet types namely, Haar wavelet, Daubechies wavelet and Newland transform.

The mother wavelet function $H(l)$ of Haar wavelet represented as

$$H(l) = \begin{cases} 1 & 0 \leq l < 0.5 \\ -1 & 0.5 \leq l < 1 \\ 0 & \text{else} \end{cases} \quad (4)$$

The scaling function $S(l)$ of mother wavelet represented as

$$S(l) = \begin{cases} 1 & 0 \leq l < 1 \\ 0 & \text{else} \end{cases} \quad (5)$$

The **Haar function** $H_{m,n}$ for every pair belonging to \mathbf{R} is

$$H_{m,n}(l) = 2^{\frac{m}{2}} H(2^m l - n), l \in \mathbf{R} \quad (6)$$

Haar function supported on the right-open interval. It has integral 0 and norm 1 in the Hilbert space $L^2(\mathbf{R})$,

$$\int_{\mathbf{R}} H_{m,n}(l) dl = 0, \|H_{m,n}\|_{L^2(\mathbf{R})}^2 = \int_{\mathbf{R}} H_{m,n}(l)^2 dl = 1 \quad (7)$$

$$\int_{\mathbf{R}} H_{m_1, n_1}(l) H_{m_2, n_2}(l) dl = \delta_{m_1, m_2} \delta_{n_1, n_2} \quad (8)$$

$\delta_{i,j}$ Represents kronecker delta.

3.2 Selection of Features Using Decision Tree

Decision tree represents decisions and decision making rules visually and explicitly. Decision trees are simple to understand and make good interpretation of data and they are the effective ways of decision making. They reduce ambiguity in decision making. Decision tree displays logic of classification for interpretation unlike neural network (NN) which uses black box algorithm [30].

A decision tree has nodes, branches, and roots to represent the classification of samples. Node represents feature (attribute), branch represents decision rule and leaf represents an outcome. A decision tree will have single root node for whole training set of data [34]. A new node is added to the tree for every partition.

The detailed steps involved in developing the decision tree are listed below:

- a) The tree starts with a node representing the training samples of data collected.
- b) If the samples are all of same class, then they are labelled as leaf.
- c) Otherwise, the algorithm will divide the samples to individual classes based on the entropy-based measure known as information gain by discretizing attribute to select optimal threshold.
- d) To create the branch, samples are portioned for each interval.
- e) The algorithm uses same steps mentioned above repeatedly to form the decision tree.
- f) This repetition process to form the tree stops only after one of the following criteria is met
 - i) When all the samples of a node given belongs to one class.
 - ii) When there is no attribute remaining to partition the samples.
 - iii) When samples get exhausted for the branch test attribute.

3.3 Classification Using Naïve Bayes Classifier

Naïve Bayes classifier (NBC) belongs to family of probabilistic classifiers, which is built on Bayes theorem of probability. It predicts the class of unknown dataset. It is simple but highly effective probabilistic learning method, applied to predictive diagnosis and other applications. The classifier relates attribute set with class variable by applying probability and statistics knowledge. The classifier learns features of training data set while analysing it [35]. [36] used Naïve Bayes algorithm to classify healthy and faulty condition of milling tool, which resulted in 96.9% classification accuracy. The algorithm assumes that all attributes (T_i) are independent when class (K) value is given.

Naïve Bayes uses following steps for classification:

- Learning conditional probability of each attribute T_i from the class label K .
- Classification is done by applying Bayes rule, to compute probability of K when T_1, \dots, T_n are given.
- The probability of a class K_i given an instance $I = \{T_1, \dots, T_n\}$ for n observations is given by:

$$p(K_i|I) = p(I|K_i) \times p(K_i)/p(I) \quad (9)$$

$$\propto p(T_1, \dots, T_n|K_i) \times p(K_i) \quad (10)$$

$$= \prod_{j=1}^n p(T_j|K_i) \times p(K_i) \quad (11)$$

where,

- $p(I)$ = probability of predictor,
- $p(K_i)$ = prior probability of the class,
- $p(K_i|I)$ = posterior probability of class(C_i) when predictor (I) is given.
- $p(I|K_i)$ = probability of predictor when class is given

It is assumed that features are independent of each other for a set of random variables. It is impossible to estimate all the parameters without such an assumption [37]. Naive Bayes is fast in response and thus, could be used for making real time predictions. It has higher success rate while classifying multi-class prediction.

4 Experimental Validation

Experiments were conducted on all geared high precision universal lathe machine powered by three-phase induction motor with cutting conditions mentioned in Tab. 1.

Oil hardened nickel steel was used as a workpiece material for the study. It is a hard steel whose chemical composition is listed in Tab. 2. It finds numerous applications in manufacturing of stamping dies, thread cutting tools, reamers and blanking tools.

Table 1: Details of cutting conditions

Work material	Oil hardened nickel steel
Tool holder	Sandvik PCLNR2020K12
Insert material	Coated carbide (diamond shape)
Cutting speed	56 m/min
Feed	0.3 mm/rev
Depth of cut	2 mm
Various conditions of tool	Healthy, overhang, worn flank and broken tool

Table 2: Chemical composition of oil hardened nickel steel

Element	C	Si	Mn	Cr	W	V	Mo	Ni	Fe
Weight percentage (%)	0.82	0.18	0.52	0.49	–	0.19	0.13	0.05	Rest

Fig. 3 shows the schematic representation of the experimental setup for understanding the acquisition and recording of cutting force and tool vibration during machining process.

Kistler dynamometer type 9257B was used to acquire cutting force during machining whose specifications are shown in Tab. 3. The Tab. 3 lists the sensitivity of the dynamometer in various directions, range of measuring the cutting force and operating temperature of the device. Dynamometer had sampling frequency of 11.6 kHz. The signal generated by the piezoelectric dynamometer flows to multi channel charge amplifier type 5070A to condition the signal. The conditioned signal flows into data acquisition system 5697A with integrated A/D card. Finally, the data is visualised on the computer screen.

Vibration signal are acquired using tri-axial accelerometer sensor (YMC145A100). The analog output of accelerometer is converted into voltage by National Instruments data acquisition (DAQ) device. Specification of the sensor are show in Tab. 4.

4.1 Experimental Procedure

Single point cutting tool was mounted on tool dynamometer, which was secured firmly on the tool post as shown in inset of Fig. 4. The direction of various force components F_x , F_y and F_z can be seen in inset of Fig. 4. Cutting conditions were set according to test plan (such as speed, feed and depth of cut). Data acquisition system was used for acquiring force signals from tool dynamometer, which was amplified by charge amplifier and sent to DynoWARE software for post processing. The force measuring system was

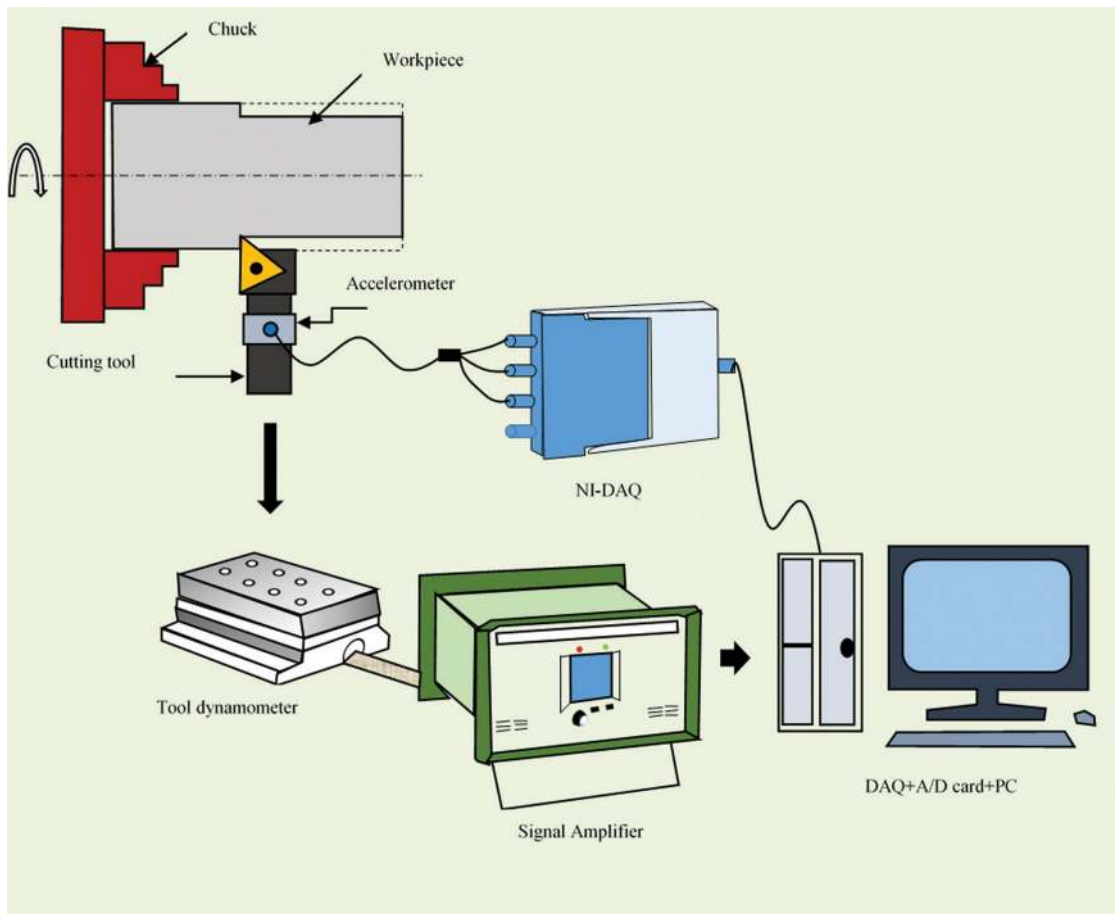


Figure 3: Schematic representation of experimental setup

Table 3: Specification of kistler 9257B dynamometer

Range F_x, F_y, F_z (kN)	Sensitivity (Pc/N)		Natural Freq. (kHz) $F_n(x, y, z)$	Capacitance (pF)	Operating Temperature Range
	F_x, F_y	F_z			
-5 to 10	-7.5	-3.7	3 to 5	220	0 to 70°C

Table 4: Specification of accelerometer used in the experimentation

Parameter	Specification
Modal Number	YMC121A100
Sensitivity (mV/g)	X:104.1 Y:99.28 Z:106.3
Measuring Range(g)	±50

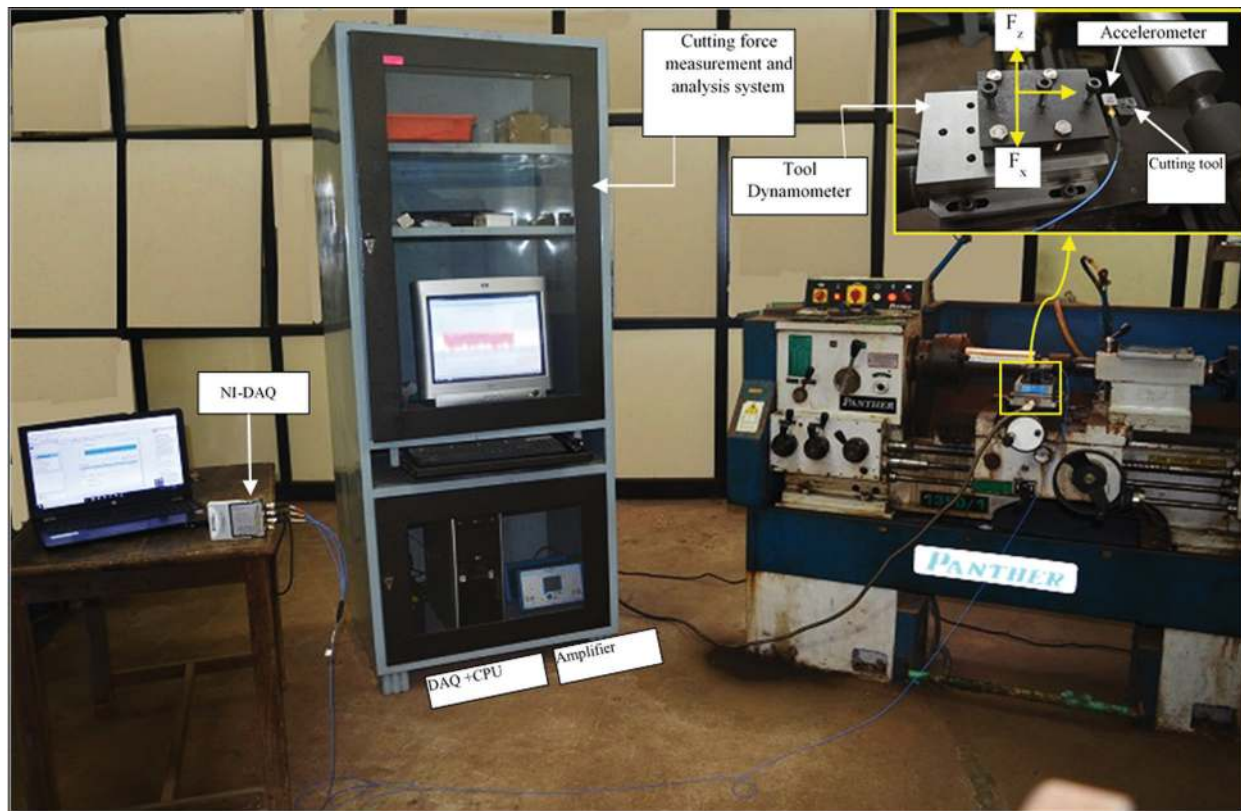


Figure 4: Experimental setup containing lathe machine with force measuring and analyzing system

calibrated prior to measurement. Rough machining was done to remove the unevenness over the workpiece and to remove the rust layer formed on the workpiece. Machining was started and measurement of cutting force for the set cutting condition and tool condition is taken. Machining time is set for 40 seconds out of which 30 second was the time for data acquisition, to allow measurement system to be stabilized prior to measurement. Tool conditions were changed keeping cutting conditions constant. The experiments were carried out for four different tool conditions. Different conditions of tool insert considered in the present study are shown in Fig. 5.

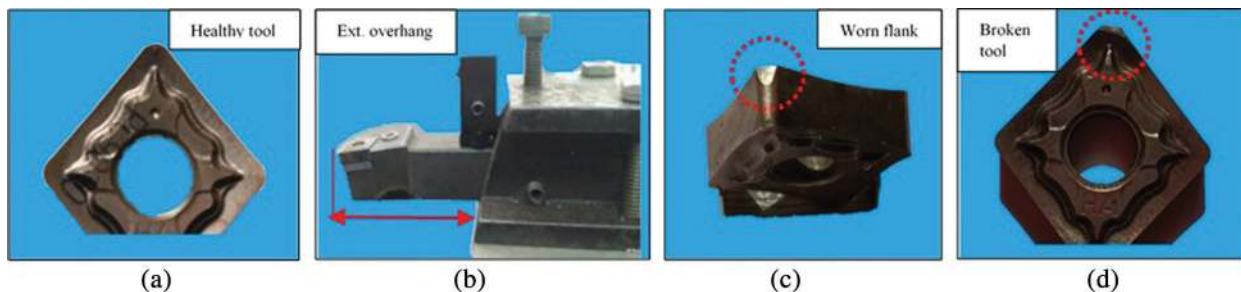


Figure 5: Photographic image of various tool wear (a) Healthy tool (b) Extended overhang (c) Worn flank (d) Broken tool

- Case 1. Healthy tool with proper mounting (Fig. 5a).
- Case 2. Healthy tool but extended overhanging (Fig. 5d).
- Case 3. Worn flank with proper mount (Fig. 5c).
- Case 4. Broken tool while mounted properly (Fig. 5b).

A fresh and brand new tool insert was used for the case 1. However, in case 2, the insert used was healthy but tool holder was extended by 45 mm extra to simulate the condition of tool mounted with extended overhang. A worn flank insert was selected in case 3. Similarly, broken tool while machining similar workpiece was chosen in case 4. Cases 1, 3 and 4 were mounted properly without extended overhang. Case 2 to case 4 are the typical tool condition experienced in machining industries.

5 Results and Discussion

The detailed discussion of results of feature extraction, feature selection and classification of the tool fault diagnosis using cutting force signal data is explained in this section.

5.1 Cutting Force Signals

Cutting force signals were recorded for healthy tool, tool with extended overhang, insert with flank wear and a broken insert at a constant cutting speed of 572 RPM, 0.3 mm/rev feed and 0.5 mm depth of cut. For each tool condition, 30 samples were recorded.

Cutting force signals acquired for various conditions of tool are shown in Figs. 6–9. The sampling frequency was 16.66 kHz. As tangential force is the major cutting force with maximum amplitude, it was considered for the analysis of machining process. Graphs in Figs. 6–9 depict the cutting force of various conditions of tool. The cutting force plotted here correspond to Z-direction. Z-direction implies tangential direction where cutting force is maximum. The effect of tool deflection due to tool failure is more prominent in tangential direction. The amplitude of peaks were changing and range of signal was also changing but it does not give any information of the tool diagnostics.

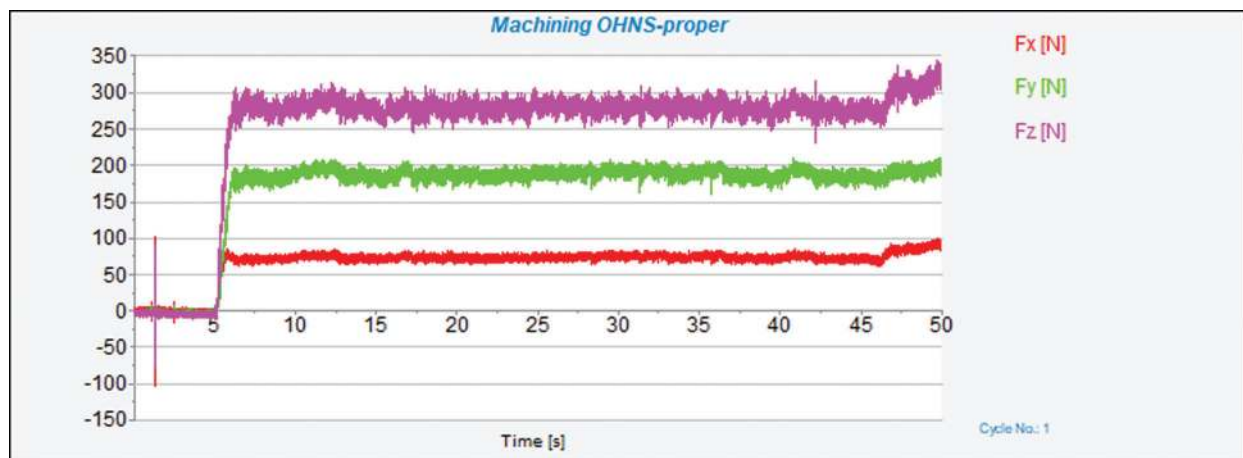


Figure 6: Time domain plot of cutting force signal of healthy tool mounted properly

Fig. 6 corresponds to healthy tool mounted properly; Fig. 7 corresponds to extended overhang. Cutting condition was maintained same for all the cases of tool state. The variations observed in signals was not significant to distinguish between proper mount and extended overhang. In such condition, it was necessary to opt for signal processing technique, which takes minor changes in signal to distinguish accurately. However, signal processing yields result pertaining to classification; if proper sensor and

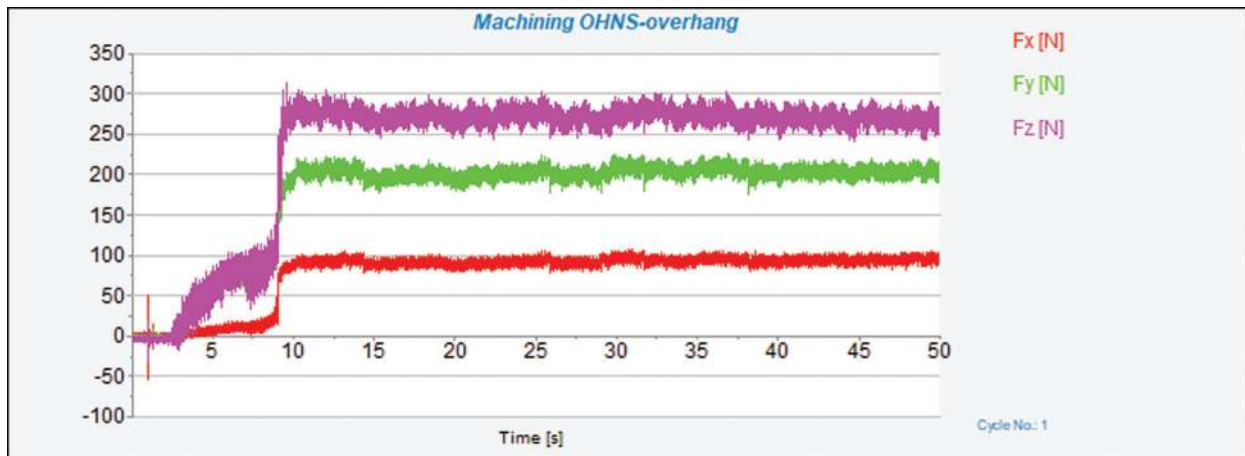


Figure 7: Time domain plot of cutting force signal of healthy tool mounted with extended overhang

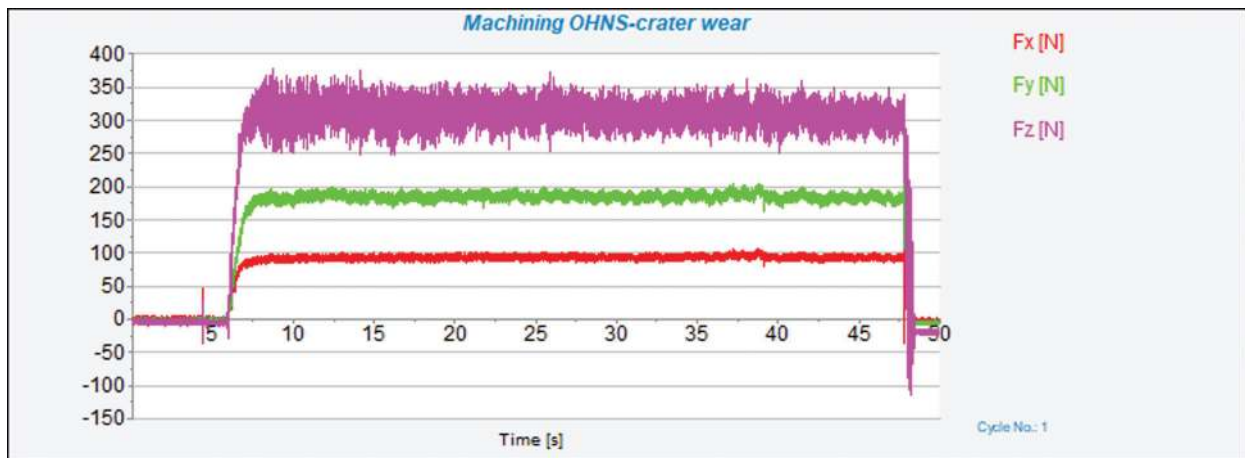


Figure 8: Time domain plot of cutting force signal of worn flank

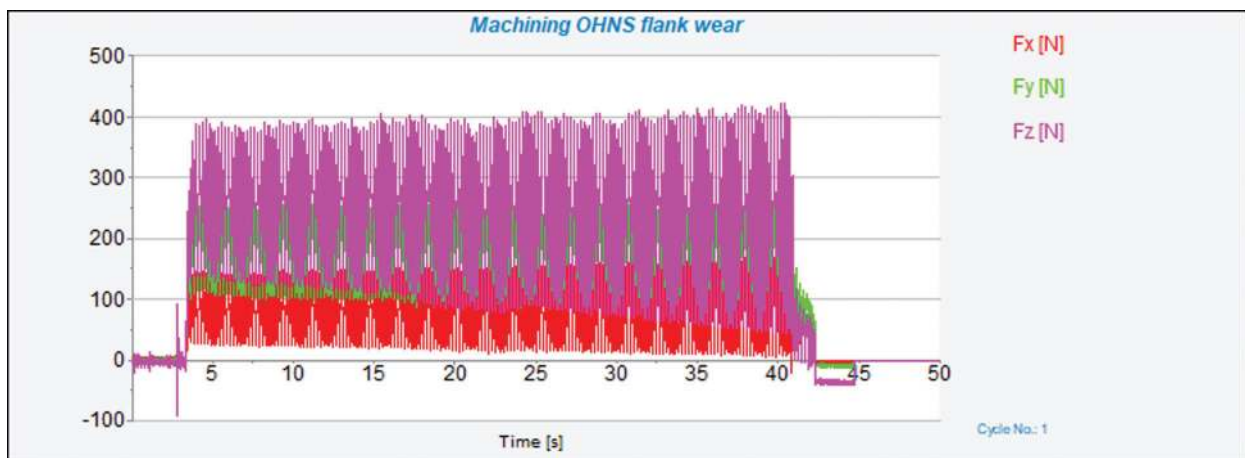


Figure 9: Time domain plot of cutting force signal of broken tool

programming is established in the system (to be monitored while machine learning makes the system learn automatically with the examples).

Fig. 8 corresponds to signal of flank wear, which induces high cutting force. Fig. 9 is the force signal for tool breakage. With tool breakage, the tool loses its geometry, rises cutting force. Pictorial representation of cutting force is not just enough to classify the tool condition. In fact, these signals have to be analysed further to get the deep information buried in the signal to classify the tool state accurately.

5.2 Tool Vibration Signal

Tool vibration was acquired using accelerometer with a sampling frequency of 25.6 kHz. The Fig. 10 shows the time domain plot of the vibration signals for various tool conditions. Preliminary observation at the signals indicate that the amplitude vibration is increasing form healthy state to overhang, then for flank wear and breakage. Such signals of various tool conditions have to be recognized by a monitoring system to contribute for a good machining.

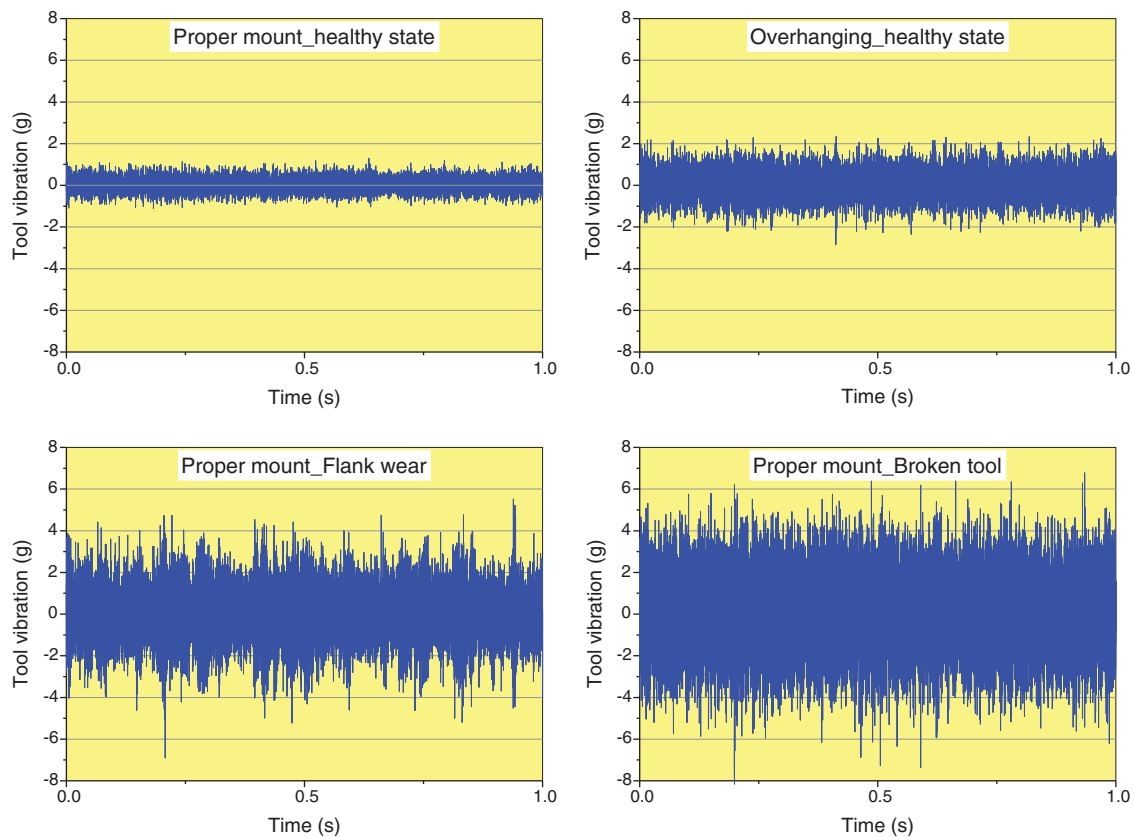


Figure 10: Time series plot of vibration signal of various tool conditions: (a) healthy tool mounted properly (b) healthy tool mounted with extended overhang (c) tool with flank wear while mounted properly (d) broken tool while mounted properly

5.3 Feature Extraction for Cutting Force Using DWT

In the current study, 'Haar' wavelet was used in the discrete wavelet transformation. The DWT extracted 8 features (V1 to V8) from each signal. There were a set of 120 signals with 30 signals for each class. The classes considered are healthy, overhang, flank wear and broken tool. Tab. 5 shows only 4 signals for each class for reference.

Table 5: Discrete wavelet features extracted from the cutting force signal

Wavelet coefficients								Tool condition/Class
V1	V2	V3	V4	V5	V6	V7	V8	
14.30	11.80	13.10	20.50	46.50	102.00	40.40	130.00	Healthy
15.40	12.00	12.70	24.00	62.00	142.00	41.60	112.00	
19.50	13.40	14.00	25.00	53.00	145.00	55.00	204.00	
17.30	13.00	14.30	23.30	52.80	123.00	66.20	183.00	
16.00	12.80	14.10	27.00	82.10	240.00	74.70	187.00	Overhang
18.00	14.40	14.70	24.50	60.10	127.00	61.20	185.00	
17.50	14.60	14.30	31.80	89.50	244.00	76.30	194.00	
16.50	14.10	13.50	24.30	55.60	111.00	51.80	158.00	
345.00	240.00	66.90	99.50	66.10	173.00	49.40	122.00	Flank wear
269.00	187.00	52.60	80.40	55.70	133.00	46.10	154.00	
199.00	141.00	41.20	65.90	70.30	197.00	57.20	141.00	
278.00	194.00	62.90	133.00	381.00	1210.00	103.00	424.00	
9.05	8.36	10.80	28.30	103.00	556.00	2700.00	19600.00	Broken tool
9.08	7.84	10.40	26.50	118.00	588.00	2930.00	21400.00	
9.19	8.32	10.50	25.20	97.60	530.00	3010.00	22400.00	
8.54	7.98	9.80	23.90	98.00	437.00	2890.00	21300.00	

Table 6: Discrete wavelet features extracted from the vibration signal

Wavelet coefficients								Tool condition/Class
V1	V2	V3	V4	V5	V6	V7	V8	
0.051	0.144	0.260	0.074	0.068	0.049	0.040	0.046	Healthy
0.050	0.142	0.271	0.073	0.069	0.043	0.037	0.048	
0.052	0.148	0.267	0.071	0.067	0.049	0.029	0.051	
0.050	0.149	0.240	0.078	0.071	0.048	0.028	0.039	
0.157	0.510	1.110	0.837	0.391	0.160	0.151	0.070	Overhang
0.151	0.486	1.090	0.932	0.365	0.157	0.149	0.091	
0.157	0.479	1.050	0.905	0.420	0.161	0.144	0.105	
0.163	0.506	1.110	0.926	0.450	0.170	0.126	0.079	
0.248	0.979	2.340	2.730	1.170	1.080	0.356	0.241	Flank wear
0.253	0.959	2.440	2.870	1.130	1.100	0.373	0.308	
0.266	1.010	2.370	3.010	1.030	0.963	0.310	0.245	
0.278	1.060	2.490	3.060	0.994	0.925	0.260	0.275	
1.980	4.770	4.150	4.750	0.901	1.250	0.441	0.337	Breakage
2.020	4.590	3.540	3.880	1.040	0.986	0.426	0.267	
2.290	4.970	3.960	4.610	1.260	1.610	0.531	0.327	
2.210	4.570	3.740	4.020	1.210	1.210	0.371	0.335	

5.4 Feature Extraction for Vibration Signal Using DWT

As like for cutting force signal, vibration signal was transformed to obtain wavelet coefficients which are tabulated in Tab. 6. The tool condition and feature extraction method remained same for vibration signal also.

5.5 Decision Tree for Feature Selection

The J48 algorithm was used to form the decision tree. The algorithm was fed with labelled wavelet coefficients to classify the classes which were derived from DWT. Out of 8 features extracted in DWT, only 6 features were used by the decision tree to classify the tool state. In decision tree, the classes are represented by rectangular boxes. The box contain number of instances classified correctly as well as instances classified incorrectly using the rule mentioned in the branch. The decision tree formed is shown in Fig. 11. All instances of flank wear were classified using single feature V3 and all instances of broken tool were classified using two features V3 and V2. Healthy and overhang were classified using 6 features with 14 branches. These two classes required more features and branches because of data similarity in both the classes. To classify flank wear feature, V3 should be greater than 15.7. To classify breakage, V3 should be less than or equal to 15.7 and V2 should be less than or equal to 9.99. Flank wear and broken tool used one and two features respectively because of their well distinguished pattern in their signal and

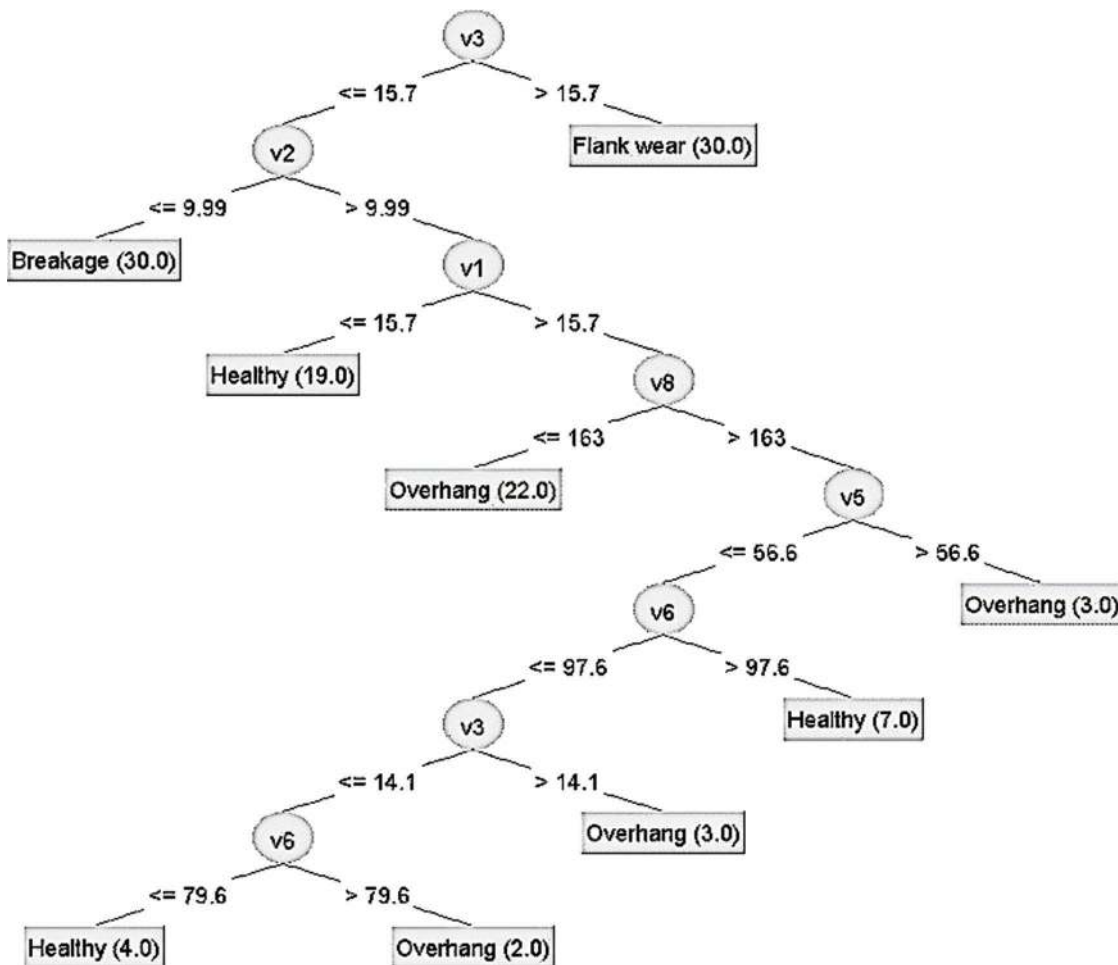


Figure 11: J48-the decision tree used for feature selection for cutting force signal

feature. However, to classify overhang and healthy, six features were used because of data overlap between them. Thus, they required feature inside feature to classify them.

Fig. 12 represent decision tree formed from the wavelet coefficients of vibration signals. In Fig. 12, V1 is the root node through which the whole tree is formed. $V1 > 0.058$ among $V1 < 0.168$ are classified as overhang else healthy or breakage. Similarly, flank wear is classified using V1, V2 and V5 and so on for rest other classes.

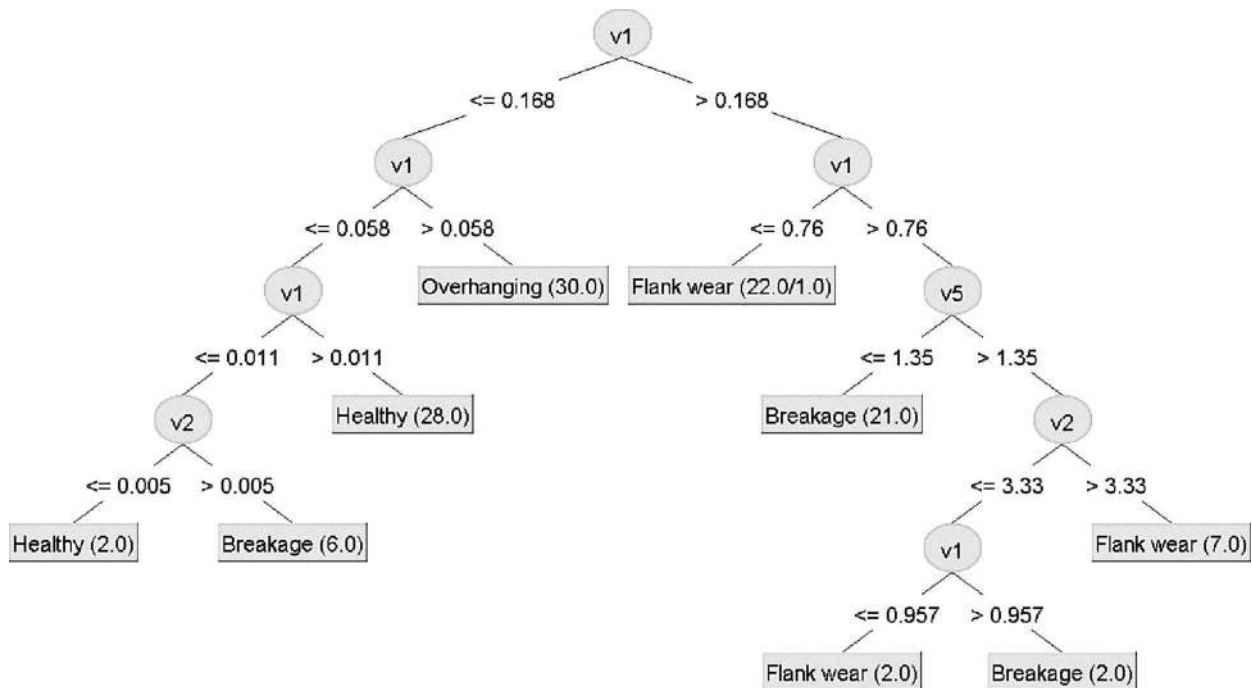


Figure 12: J48 decision tree for vibration signal

5.6 Classification Using Naïve Bayes Algorithm for Cutting Force

Naïve Bayes algorithm used 10 fold cross validation method, with 66% training data set and 34% testing data set. Confusion matrix tabulated in Tab. 7 represents the number of instances being classified into classes. Across the row are classes and down the column are the classes, being classified into various classes. Referring to first row, out of 30 instances of a healthy class 29 were classified as healthy, one was misclassified as overhang. Referring to second row, 27 out of 30 were correctly classified as overhang while 3 were misclassified as healthy. Referring to third row, all instances of flank wear were correctly classified as flank wear. Referring to fourth row all instances of broken tool classified correctly.

Table 7: Confusion matrix for Naive Bayes classifier

Classified as →	Healthy	Overhang	Flank wear	Broken tool
Healthy	29	1	0	0
Overhang	3	27	0	0
Flank wear	0	0	30	0
Broken tool	0	0	0	30

Referring to [Tab. 8](#), the terms used in the table are briefed as follows: True Positives (TP) are fractions of instances that are correctly classified into their respective classes. False Positives (FP) are fractions of instances that are wrongly classified into other classes. Precision for a class is the number of True Positives divided by the number of True Positives and False Positives in that class.

5.7 Classification Using Naive Bayes for Vibration Signal

Following [Tab. 9](#) shows the confusion matrix for vibration signal where in which Naïve Bayes classified tool faults using vibration signal at 70% accuracy. i.e., 84/120 were correctly classified to their respective classes, 36/120 were misclassified to other classes. This misclassification is due to data similarity in both classes and also inefficient classification algorithm.

[Tab. 10](#) tabulates the detailed classification accuracy chart formed by Naïve Bayes algorithm for vibration signals.

Table 8: Detailed classification accuracy chart for Naive Bayes algorithm

Class	TP Rate	FP Rate	Precision	Recall	F-Measure	ROC Area
Healthy	0.967	0.033	0.906	0.967	0.935	0.996
Overhang	0.9	0.011	0.964	0.9	0.931	0.996
Flank wear	1	0	1	1	1	1
Broken tool	1	0	1	1	1	1
Weighted avg.	0.967	0.011	0.968	0.967	0.967	0.998

Table 9: Confusion matrix for Naive Bayes classifier for vibration signal

Classified as →	Proper	Overhang	Flank wear	Breakage
Proper	30	0	0	0
Overhang	0	30	0	0
Flank wear	0	0	6	24
Breakage	6	0	6	18

Table 10: Detailed classification accuracy chart for Naive Bayes algorithm for vibration signal

Class	TP Rate	FP Rate	Precision	Recall	F-Measure	ROC Area
Proper	1	0.067	0.833	1	0.909	0.996
Overhang	1	0	1	1	1	1
Flank wear	0.2	0.067	0.5	0.2	0.286	0.896
Breakage	0.6	0.267	0.429	0.6	0.5	0.833
Weighted avg.	0.7	0.1	0.69	0.7	0.674	0.931

6 Conclusions

In this article, fault diagnosis of carbide tool inserting with healthy and simulated faults were carried out. Extended overhang, worn flank and broken tool were the faulty conditions considered for the current study.

Tool fault diagnosis was carried out using vibration and cutting force signal. Discrete wavelet features were extracted through discrete wavelet transformation from the acquired vibration and cutting force signals. The transformation yielded 8 features, V1 to V8 for each signal. Significant features, which give relevant information about different classes of tool condition, were selected by using J48 algorithm. The tree selected 6 features out of 8 as significant for cutting force signal and 3 features for vibration signal. Naïve Bayes algorithm was used to classify the faulty condition of the tool. 10 fold cross validation was used to train the algorithm. The algorithm was trained with 66% of total data and remaining 34% as testing data. Naïve Bayes algorithm classified the instances with 96.667% accuracy using cutting force signal while 70% accuracy using vibration signal. Very characteristic pattern in cutting force signal makes it possible to classify tool faults effectively. Hence, cutting force signals are best signals for fault diagnosis in comparison to vibration signals.

Funding Statement: The author(s) received no specific funding for this study.

Conflicts of Interest: The authors declare that they have no conflicts of interest to report regarding the present study.

References

1. Johansson, D., Häggglund, S., Bushlya, V., Ståhl, J. (2017). Assessment of commonly used tool life models in metal cutting. *Procedia Manufacturing*, 11, 602–609.
2. Masood, I., Jahanzaib, M., Haider, A. (2016). Tool wear and cost evaluation of face milling grade 5 titanium alloy for sustainable machining. *Advances in Production Engineering and Management*, 11(3), 239–250. DOI 10.14743/apem2016.3.224.
3. Yesilyurt, I., Ozturk, H. (2007). Tool condition monitoring in milling using vibration analysis. *International Journal of Production Research*, 45(4), 1013–1028. DOI 10.1080/00207540600677781.
4. El-Wardany, T. I., Gao, D., Elbestawi, M. A. (1996). Tool condition monitoring in drilling using vibration signature analysis. *International Journal of Machine Tools and Manufacture*, 36(6), 687–711. DOI 10.1016/0890-6955(95)00058-5.
5. Ghule, G., Ambhore, N. H., Chinchankar, S. (2017). Tool condition monitoring using vibration signals during hard turning: a review. *International Conference on Advances in Thermal Systems, Materials and Design Engineering, Mumbai*, <https://ssrn.com/abstract=3101977>.
6. Ertunc, H. M., Oysu, C. (2004). Drill wear monitoring using cutting force signals. *Mechatronics*, 14(5), 533–548. DOI 10.1016/j.mechatronics.2003.10.005.
7. Jemielniak, K., Arrazola, P. (2008). Application of AE and cutting force signals in tool condition monitoring in micro-milling. *CIRP Journal of Manufacturing Science and Technology*, 1(2), 97–102. DOI 10.1016/j.cirpj.2008.09.007.
8. Li, X., Djordjevich, A., Venuvinod, P. K. (2000). Current-sensor-based feed cutting force intelligent estimation and tool wear condition monitoring. *IEEE Transactions on Industrial Electronics*, 47(3), 697–702. DOI 10.1109/41.847910.
9. Huynh, V. M., Fan, Y. (1992). Surface-texture measurement and characterisation with applications to machine-tool monitoring. *International Journal of Advanced Manufacturing Technology*, 7(1), 2–10. DOI 10.1007/BF02602945.
10. Kus, A., Isik, Y., Cakir, M. C., Coşkun, S., Özdemir, K. (2015). Thermocouple and infrared sensor-based measurement of temperature distribution in metal cutting. *Sensors*, 15(1), 1274–1291. DOI 10.3390/s150101274.
11. Ram, K. R., Shankar, N. A., Vidyasagar, P., Senthil, G. S. (2017). Analysis of tool wear using machine vision system. *International Advanced Research Journal in Science, Engineering and Technology ISO 3297:2007 Certified*, 4(6), 7–10.
12. Alan, V. O., Ronald, W. S., John, R. (1989). *Discrete-time signal processing*. New Jersey: Prentice Hall Inc.

13. Jurkovic, J., Korosec, M., Kopac, J. (2005). New approach in tool wear measuring technique using CCD vision system. *International Journal of Machine Tools and Manufacture*, 45(9), 1023–1030. DOI 10.1016/j.ijmachtools.2004.11.030.
14. Uehara, K., Ryabov, O., Mori, K., Kasashima, N. (1996). An in-process direct monitoring method for milling tool failures using a laser sensor. *CIRP Annals-Manufacturing Technology*, 45(1), 97–100.
15. Schmitt, R., Cai, Y., Pavim, A. (2012). Machine vision system for inspecting flank wear on cutting tools. *ACEEE International Journal on Control System and Instrumentation*, 03(01), 13.
16. Ramirez-Nunez, J. A., Trejo-Hernandez, M., Romero-Troncoso, R. J., Herrera-Ruiz, G., Osornio-Rios, R. A. (2018). Smart-sensor for tool-breakage detection in milling process under dry and wet conditions based on infrared thermography. *International Journal of Advanced Manufacturing Technology*, 97(5–8), 1753–1765. DOI 10.1007/s00170-018-2060-4.
17. Dimla, E. D. (2000). On-line metal cutting tool condition monitoring. I : force and vibration analyses. *International Journal of Machine Tools and Manufacture*, 40(5), 739–768. DOI 10.1016/S0890-6955(99)00084-X.
18. Hesser, D. F., Markert, B. (2019). Tool wear monitoring of a retrofitted CNC milling machine using artificial neural networks. *Manufacturing Letters*, 19, 1–4. DOI 10.1016/j.mfglet.2018.11.001.
19. Liu, C., Li, Y., Zhou, G., Shen, W. (2018). A sensor fusion and support vector machine based approach for recognition of complex machining conditions. *Journal of Intelligent Manufacturing*, 29(8), 1739–1752. DOI 10.1007/s10845-016-1209-y.
20. Bhuiyan, M. S. H., Choudhury, I. A., Dahari, M. (2014). Monitoring the tool wear, surface roughness and chip formation occurrences using multiple sensors in turning. *Journal of Manufacturing Systems*, 33(4), 476–487. DOI 10.1016/j.jmsy.2014.04.005.
21. Plaza, E. G., López, P. J. N. (2017). Surface roughness monitoring by singular spectrum analysis of vibration signals. *Mechanical Systems and Signal Processing*, 84, 516–530. DOI 10.1016/j.ymsp.2016.06.039.
22. Salgado, D. R., Alonso, F. J., Cambero, I., Marcelo, A. (2009). In-process surface roughness prediction system using cutting vibrations in turning. *International Journal of Advanced Manufacturing Technology*, 43(1–2), 40–51. DOI 10.1007/s00170-008-1698-8.
23. Kannatey-asibu, E., Yum, J., Kim, T. H. H. (2017). Monitoring tool wear using classifier fusion. *Mechanical Systems and Signal Processing*, 85, 651–661. DOI 10.1016/j.ymsp.2016.08.035.
24. Cuka, B., Kim, D. (2017). Robotics and computer-integrated manufacturing fuzzy logic based tool condition monitoring for end-milling. *Robotics and Computer Integrated Manufacturing*, 47, 22–36. DOI 10.1016/j.rcim.2016.12.009.
25. Sugumaran, V., Muralidharan, V., Ramachandran, K. I. (2007). Feature selection using decision tree and classification through proximal support vector machine for fault diagnostics of roller bearing. *Mechanical Systems and Signal Processing*, 21(2), 930–942. DOI 10.1016/j.ymsp.2006.05.004.
26. Elangovan, M., Devasenapati, S. B., Sakthivel, N. R., Ramachandran, K. I. (2011). Evaluation of expert system for condition monitoring of a single point cutting tool using principle component analysis and decision tree algorithm. *Expert Systems with Applications*, 38(4), 4450–4459. DOI 10.1016/j.eswa.2010.09.116.
27. Indira, V., Vasanthakumari, R., Sugumaran, V. (2010). Expert systems with applications minimum sample size determination of vibration signals in machine learning approach to fault diagnosis using power analysis. *Expert Systems with Applications*, 37(12), 8650–8658. DOI 10.1016/j.eswa.2010.06.068.
28. Wang, Q., Garrity, G. M., Tiedje, J. M., Cole, J. R. (2007). Naïve Bayesian classifier for rapid assignment of rRNA sequences into the new bacterial taxonomy. *Applied and Environmental Microbiology*, 73(16), 5261–5267. DOI 10.1128/AEM.00062-07.
29. Amarnath, M., Sugumaran, V., Kumar, H. (2013). Exploiting sound signals for fault diagnosis of bearings using decision tree. *Measurement*, 46(3), 1250–1256. DOI 10.1016/j.measurement.2012.11.011.
30. Sugumaran, V., Jain, D., Amarnath, M., Kumar, H. (2013). Fault diagnosis of helical gear box using decision tree through vibration signals. *International Journal of Performability Engineering*, 9(2), 221–233.
31. Kumar, H., Sugumaran, V., Amarnath, M. (2016). Fault diagnosis of bearings through sound signal using statistical features and bayes classifier. *Journal of Vibration Engineering and Technologies*, 4(2), 87–96.

32. Madhusudana, C. K., Budati, S., Gangadhar, N., Kumar, H., Narendranath, S. (2016a). Fault diagnosis studies of face milling cutter using machine learning approach. *Journal of Low Frequency Noise, Vibration and Active Control*, 35(2), 128–138. DOI 10.1177/0263092316644090.
33. Sundararajan, D. (2015). *Discrete wavelet transform: a signal processing approach*. John Wiley & Sons Singapore Pte. Ltd. DOI 10.1002/9781119113119.
34. Anoop, P. S., Sugumaran, V. (2017). Classifying machine learning features extracted from vibration signal with logistic model tree to monitor automobile tyre pressure. *Structural Durability & Health Monitoring*, 11(2), 191–208.
35. Vernekar, K., Kumar, H., Gangadharan, K. V. (2017). Engine gearbox fault diagnosis using empirical mode decomposition method and Naïve Bayes algorithm. *Sadhana-Academy Proceedings in Engineering Sciences*, 42(7), 1143–1153.
36. Madhusudana, C. K., Gangadhar, N., Kumar, H., Narendranath, S. (2014). Use of discrete wavelet features and support vector machine for fault diagnosis of face milling tool. *Structural Durability & Health Monitoring*, 12(2), 97–113.
37. Espinilla, M., Montero, J., Rodríguez, J. T. (2014). Computational intelligence in decision making. *International Journal of Computational Intelligence Systems*, 7(Suppl. 1), 1–5. DOI 10.1080/18756891.2014.853925.